A Solar Radiation Model for Sub-Arctic Woodlands

R. G. WILSON AND D. E. PETZOLD
Dept. of Geography, McGill University, Montreal, Quebec, Canada

(Manuscript received 7 July 1973)

ABSTRACT

A mathematical model is presented which is used to calculate the flux of solar radiation to a melting snowpack in sub-arctic woodlands. Using tree height, branch radius, and distance between trees as input data, the model calculates both hemispherical and angular view factors. The latter are checked by a special photographic technique and good agreement is obtained. The view factors are used in conjunction with measurements of global and diffuse solar radiation at a base station to calculate the corresponding fluxes in nearby woodland. A test of the model at Schefferville, Quebec, showed that calculated and observed values were highly correlated, although the model consistently produced slight underestimates.

1. Introduction

The physical nature of a forest strongly affects the supply of radiant energy at a melting snowpack. Trees absorb some of the incoming solar radiation so that the flux to the snow surface is less than that in the open. However, the snow in the forest will usually receive more long-wavelength radiation since the trees have a higher effective radiating temperature than the clouds and sky above. The net result of these opposing effects clearly depends upon the physical structure and density of the forest, and they should be accounted for in any systematic determination of the radiation balance of snow in forested regions.

The transfer of radiation through forest canopies has received considerable study but there have been few treatments of the effects of structure and density. The radiation balance equation presented by the U. S. Army Corps of Engineers (1956), probably the best known of these, accounts only for variations in crown coverage. This forest density parameter, when expressed as a decimal fraction and subtracted from unity, gives an approximate measure of the proportion of the sky seen by the snow surface. However, the use of such a total-sky view factor applies only when the incoming radiation originates equally from all parts of the sky. Diffuse solar and longwave sky radiation usually are considered to be isotropic and could be calculated in this manner, but the technique does not apply to direct solar radiation which has a variable influence according to solar elevation. The latter is considered in radiation models presented by Federer (1971) and Reifsnyder *et al.* (1971). These are based on the concept of a forest canopy which has a uniform effect on radiation penetration, and can be applied best to closed canopies typical of mature middle-latitude and tropical forests.

Sub-arctic woodlands, which are spruce-dominated, tend to have an open structure so the problem of radiation penetration is simplified somewhat. As shown in Fig. 1, a large proportion of the sky is visible overhead so it can be assumed that the diffuse solar radiation reaching the snow originates primarily from the sky, rather than from the scattering of direct radiation by the tree branches and needles. This is analogous to the case of a middle-latitude forest clearing and can be approached in the same way. Following Reifsnyder and Lull (1965), the diffuse radiation in the woodland can be calculated by using a hemispherical view factor P which represents the proportion of the sky's hemisphere which is not covered by trees.

The direct solar radiation can be calculated in a similar manner, since the spiked crowns stand out individually, and the occurrence of shade depends on whether or not a tree spike intersects the path of the

FIG. 1. A photograph of the test site.

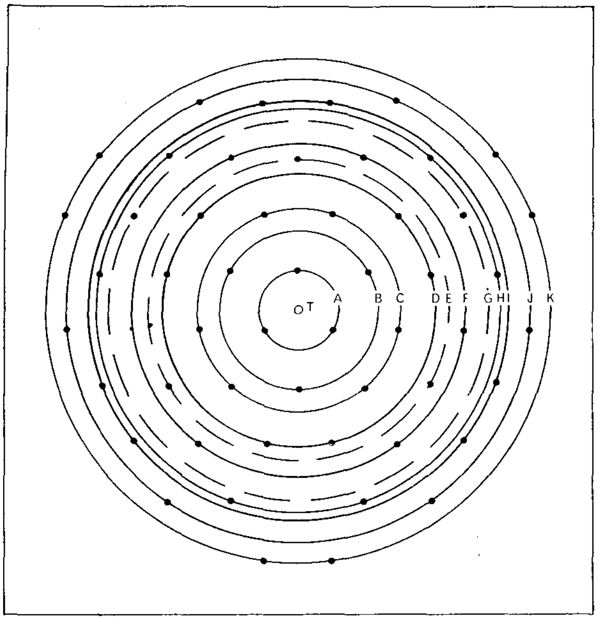

FIG. 2. Plan of theoretical woodland.

sun. Thus, for any given solar elevation one can define an angular view factor S which represents the proportion of sky not covered by tree vegetation at that particular angle.

Ignoring reflection from the trees, the total solar radiation reaching the snow surface in the woodland is given by

$$K_f = QS + qP, \tag{1}$$

where Q and q are the direct and diffuse solar radiation fluxes, respectively, as measured outside the woodland. The long-wavelength fluxes can be calculated in a similar manner using P as the only vegetation parameter, but this paper will be concerned only with solar radiation calculations.

The approach described above is being used to study snowmelt in sub-arctic woodlands near Schefferville, Quebec (54°43′N, 67°42′W). Various radiation fluxes are measured at the McGill Sub-Arctic Research Laboratory, and are being mapped for the surrounding woodlands, where S and P values have been determined. FitzGibbon and Dunne (1973) have shown how a photographic technique can be used to find the view factors and this paper describes a mathematical model devised for the same purpose.

2. Model to determine view factors

The model uses three inputs: mean tree height; mean radius of branches, including trunk, near the ground or snow level; and mean distance between trees. The woodland is assumed to consist of equi-distant trees, all of which conform to the standard structure. View factors are calculated for an observation point T mid-way between three trees as illustrated in Fig. 2. The central idea of the procedure is to project images of the trees onto a hypothetical cylinder passing through the trunks of the three nearest trees (labelled A in Fig. 2), and then finding the total length of branches at any given angle of elevation.

The theoretical woodland consists of sets of trees, labelled A to K in Fig. 2, in which all trees in any set are at an equal distance from point T. These distances can be calculated as functions of the mean distance Y between trees as summarized in Table 1 and as shown graphically in Fig. 3. Sets A, B, E and G each contain three trees while the rest contain six trees each. Due to the regularity of the spacing, the trees at E and G are not visible from point T, so they are not considered in subsequent calculations.

The image projection is begun by choosing m angular elevations $(a_i = a_1, a_2, \ldots, a_m)$ for which the calculations will be performed. So, for example, if a 2° increment has been chosen, then $a_1 = 2°$, $a_2 = 4°$, etc. The trees are then divided into vertical segments according to elevation, and the height increment h_n in the nth segment is determined as

$$h_n = x \tan a_n - \sum_{i=1}^{n-1} h_i, \tag{2}$$

where x is the distance to that particular tree. Calculation of (2) is repeated until the sum of the height increments exceeds the mean actual tree height Z.

The next step is to find the radius of the tree branches at the top of each vertical segment. It has been assumed here that the radius changes logarithmically with height, such that the radius r_n at the top of the nth segment is given by

$$r_n = R_x' \log_{10}[11 - 10(\sum_{i=1}^{n} h_i/Z)], \tag{3}$$

where R_x' is the apparent branch radius near ground level projected onto the hypothetical cylinder at distance A, such that for a tree at distance x

$$R_x' = RA/x, \tag{4}$$

where R is the actual mean radius.

TABLE 1. Distances to trees from point of observation T, as a function of mean distance Y between trees.

Tree	Distance
A	$0.5Y/\cos 30$
B	$Y/\cos 30$
C	$B^2 + Y^2$
D	$(0.5Y)^2 + (B + Y\cos 30)^2$
E	not seen
F	$(1.5Y)^2 + (B + Y\cos 30)^2$
G	not seen
H	$(3Y)^2 + A^2$
I	$(2.5Y)^2 + (B + Y\cos 30)^2$
J	$(3.5Y)^2 + (0.5Y\tan 30)^2$
K	$(0.5Y)^2 + (B + 3Y\cos 30)^2$

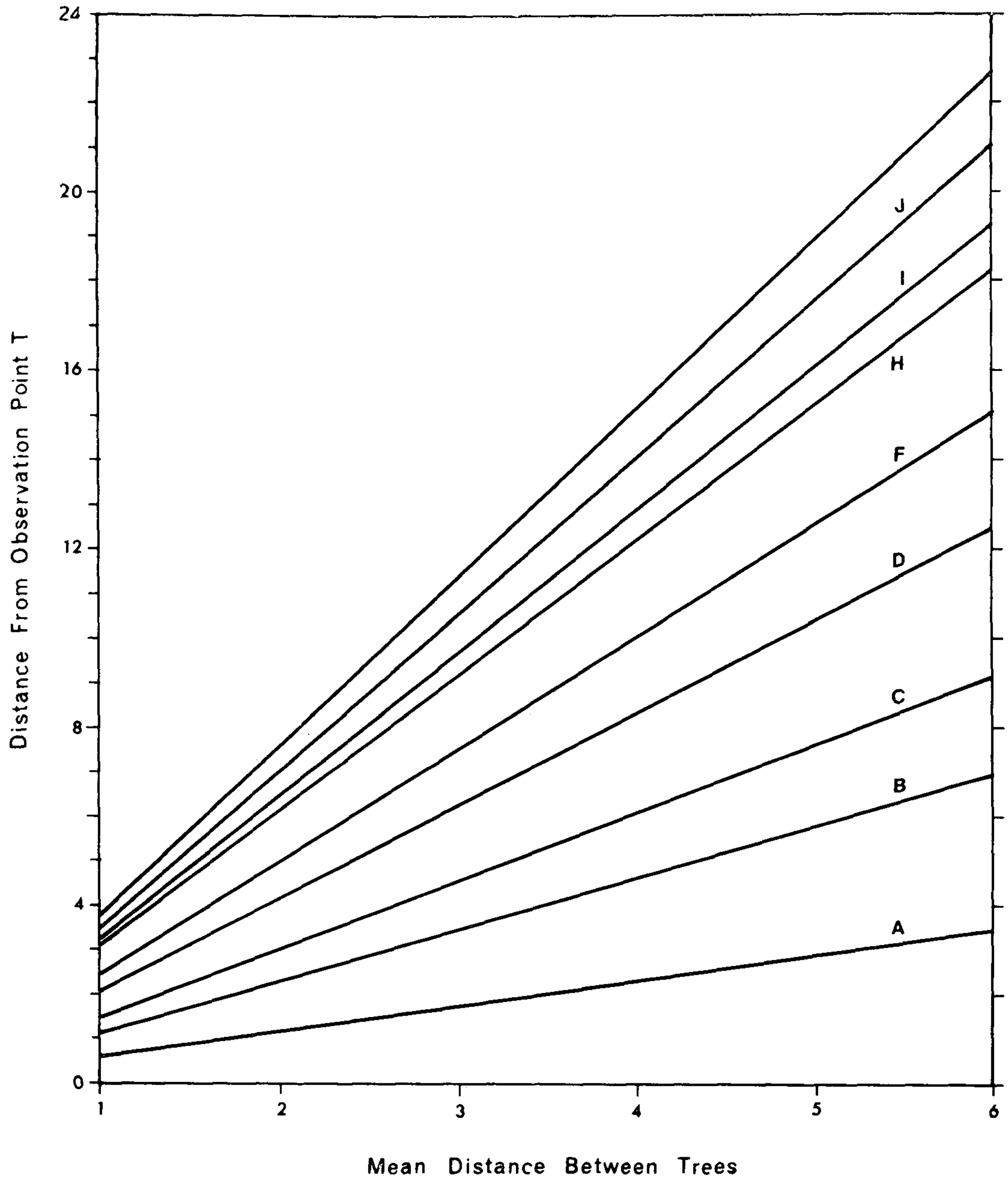

FIG. 3. Distances to trees from observation point T as a function of mean distance between the trees.

The logarithmic profile of (3) was chosen originally because field observations indicated that healthy trees in this region most often conform to this general shape. View factors have also been calculated using a triangular profile but these do not agree as well with the photograph analyses. It is important to note that (3) gives $r=R'$ when the sum of the height increments represent one-tenth of the full tree height, so that, strictly speaking, R should be measured at this height. However, the exact point of measurement is relatively unimportant, since (3) gives very small changes near the ground.

Repetition of the calculations in (2)–(4) produces a matrix of radii, for all angular elevations and all distances, as they would be observed on the cylinder at A. For any given elevation and distance, the width w of the projected trees is given by

$$w=2rN, \tag{5}$$

where N is the number of trees at that particular distance. The total width of all projected trees at the nth elevation increment is thus

$$w_n=6r_A+6r_B+12r_C+12r_D+12r_F+12r_H+12r_I+12r_J, \tag{6}$$

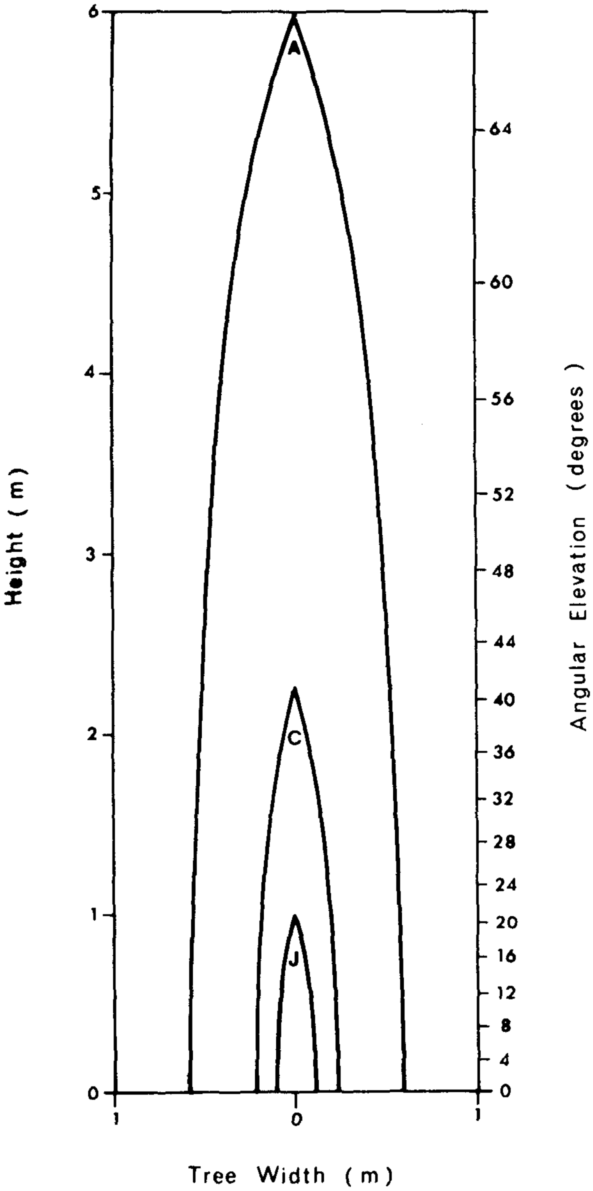

FIG. 4. Images of trees at distances A, C and J when $H=6.0$ m, $R=0.6$ m and $Y=4.5$ m.

and the angular view factor S is defined as the proportion of the cylinder circumference not covered by trees, so that at elevation a_n the view factor S_n is determined as

$$S_n = 1 - \frac{w_n}{2\pi A}, \tag{7}$$

where A is the radius of the hypothetical cylinder.

The summation of radii in (6) has been terminated at distance J because it has been found that this produces the best results in comparison to photograph analysis for five sites. This arbitrary decision could be eliminated by making allowance for the overlapping of tree branches, but in the present case, the model has been kept as simple as possible. In the existing form, it matters little whether the calculation is stopped at I, J or K because, as shown in Fig. 4, images of trees at these distances are very small and S is affected only near the horizon.

The hemispherical view factor can be found by numerically integrating the area of trees on the cylinder, and then calculating the proportion of the total hemisphere of the sky which is not covered by trees. One way of doing this is to calculate the effective height Z' of a solid mass of tree vegetation as given by

$$Z' = \sum_{i=1}^{m} [(1-S_i)h_A], \tag{8}$$

where h_A represents the height increment at distance A, and m is the total number of increments. The hemispherical view factor P according to Reifsnyder and Lull (1965) is then

$$P = \sin^2\left(\tan^{-1}\frac{A}{Z'}\right). \tag{9}$$

3. Experimental procedure

Total solar radiation was measured at an open lichen woodland site near Wishart Creek, 5 mi southeast of Schefferville, from 8 May to 7 June, 1972. Each of five Lintronic solarimeters was mounted on a base 1 m above the snow (Fig. 1), and these were placed randomly among the trees. The solarimeters were connected in series, and the resulting signal was recorded on one channel of a Honeywell 194 2-pen strip-chart recorder. The second channel recorded the signal from a Kipp and Zonen solarimeter installed on an open hill about 100 m from the woodland site. An ac power supply for the recorder was provided by a Heath MP 10 inverter attached to a car battery. The Lintronic solarimeters were calibrated immediately at the end of the measurement period so the temperature effects on the calibration coefficients would be minimized. Using the temperature coefficient of -0.2% $(°C)^{-1}$ given by the manufacturer, the calibration of the instruments would have changed by 2.7% during the experimental period. This was considered to be well within the required accuracy, so the data were not adjusted for temperature variations.

Radiation measurements from the McGill Sub-Arctic Research Laboratory in Schefferville have been used here to provide values of Q and q for (1). Total solar radiation $(Q+q)$ was measured at the laboratory with an Eppley 8-48 solarimeter, and diffuse solar was measured with a Kipp and Zonen solarimeter installed beneath a shadow band similar to that described by Horowitz (1969).

Tree dimension data for the woodland site were collected after the snow had melted by measuring all trees within a 930 m² area. The trees were found to

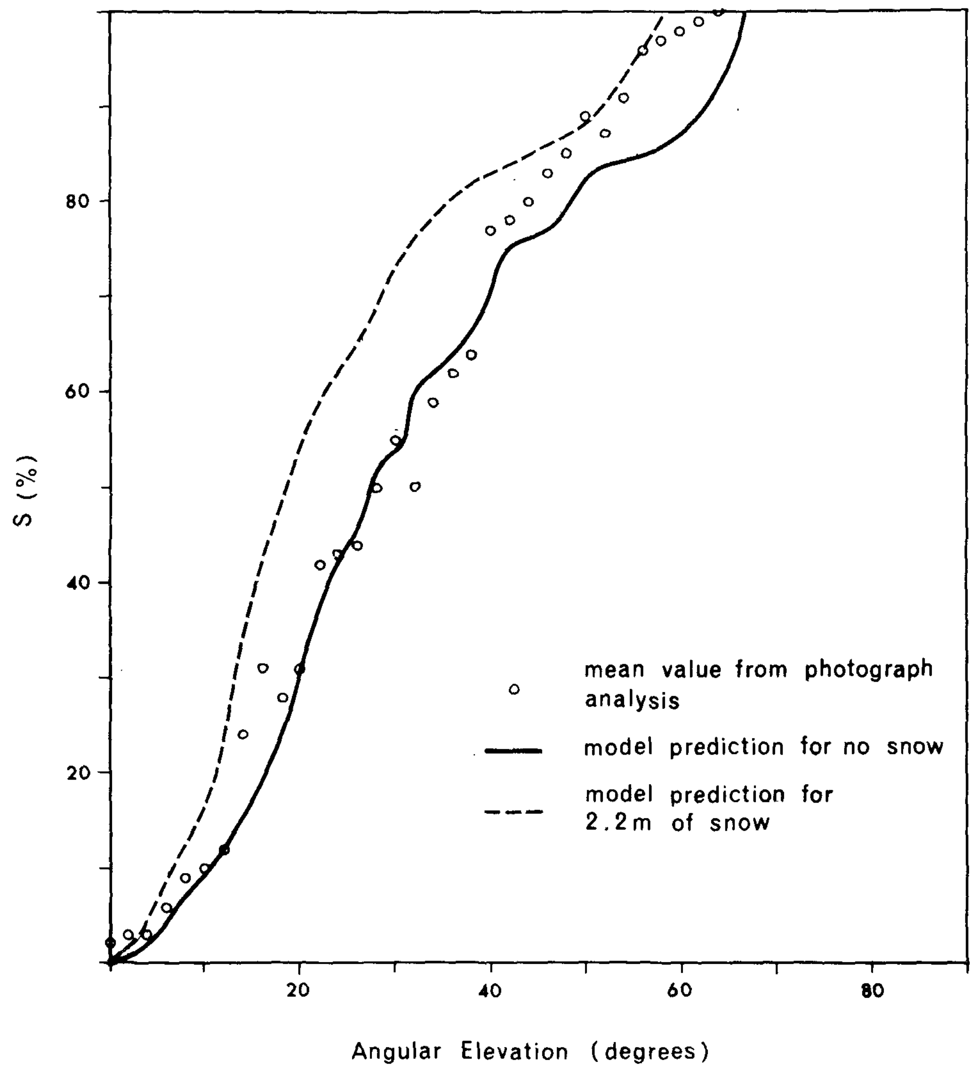

FIG. 5. The variation of S with angular elevation as calculated by the model and by photograph analysis.

have an average height of 6.2 m, and an average branch radius of 0.61 m near the ground. The mean distance between trees averaged 4.5 m and crown coverage of the plot was 6%.

Special photographs were taken to provide control values of S. The technique, described by FitzGibbon and Dunne (1973), utilizes a Horizont Panoramic camera with a lens mounted in a turret. Rotation of the turret provides a 70° by 120° angle of view with a minimum of distortion. A small wooden ramp with a slope of 30° was constructed to hold the camera on the ground, so that when it was facing upward the traverse of the lens would start at a horizontal position and finish 30° past the zenith. After the first shot, the ramp and camera were rotated through 180° so that the two resulting photographs overlapped and provided a strip sample of the forest structure. This procedure was repeated so that a total of four photographs (two strips) were obtained for the site. These were analyzed at 2° intervals from ground level by counting the number of arbitrary units in which sky was visible. The value of S at any interval was determined as the ratio of the number of units of sky to the total number of units across the photograph.

4. Results

A comparison of S values determined by calculation and by photograph analysis for the test site (Fig. 5) reveals good agreement, except for a region near the tops of the trees where the calculated values are slightly smaller. This feature has also appeared in similar tests for other sites, and may indicate a deviation from the assumed logarithmic profile near the tree tops, and it might also be caused by the presence of only a few trees with greater than average height. To test the model's radiation predictions, the S values were recalculated to

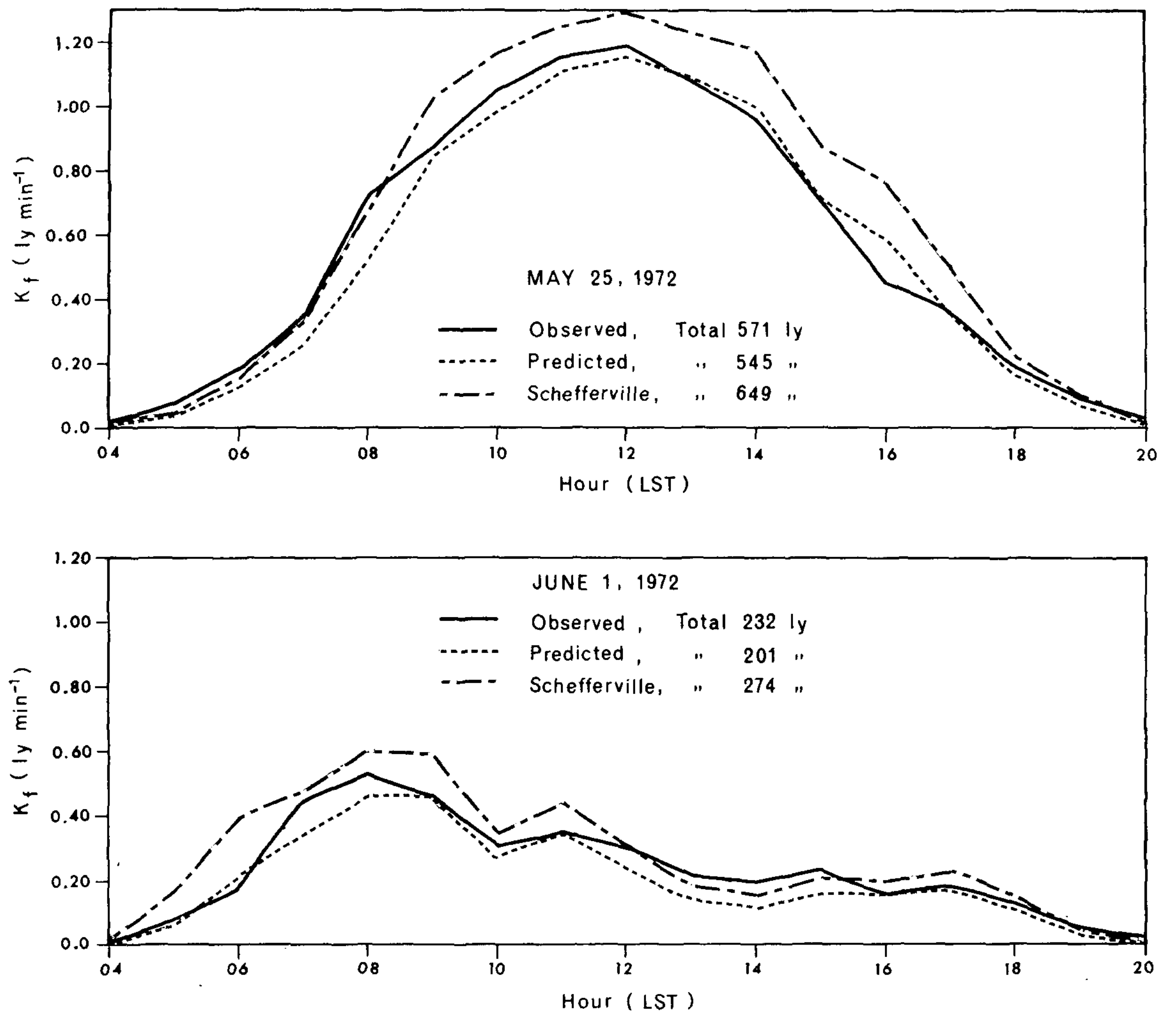

FIG. 6. Predicted and observed values of solar radiation for a sunny day (top) and a cloudy day (bottom).

allow for the height of the solarimeters above the snow (1 m) and for the varying snow depth (1.2 m on 8 May to 0.3 m on 7 June). The revised curve for an equivalent of 2.2 m of snow on 8 May reveals increases in the S values of 15–20% at most elevations, and the hemispherical view factor increased from $P=0.66$ for no snow to $P=0.83$ for 2.2 m of snow.

Predicted and observed values of solar radiation in the forest for typical sunny and cloudy days are shown in Fig. 6, together with the corresponding values measured at the laboratory. The agreement between the forest values is generally good, but two significant points emerge: 1) there is an asymmetrical pattern in the difference on the clear day, and 2) the prediction was nearly always too low on the cloudy day. The first can be attributed to an asymmetric distribution of trees around the measurement site; trees in the southwest sector were taller and were grouped closer than those toward the east, and this resulted in an under-prediction in the morning and an over-prediction in the afternoon.

The error in the diffuse prediction could have arisen in several ways. First, the calculated S values were too small near the tree tops and this would have produced a corresponding effect on P. Second, some error would be introduced by the assumption that the diffuse radiation is isotropic, although this would be minimized under the overcast conditions shown in Fig. 6b. Third, there would be some penetration of radiation through the tree vegetation which is considered to be opaque in the model. This element could be eliminated as a consistent source of error by empirically determining a transmission coefficient, but it is felt that such an extension of the analysis is not justified on the basis of the data from this one site. Finally, an error might have been introduced by the choice of sampling locations among the trees. The low radiation predictions of the model cannot be attributed to the location of point T since this particular observation point receives the maximum amount of radiation available in the woodland. The field measurements might have been biased in favor of

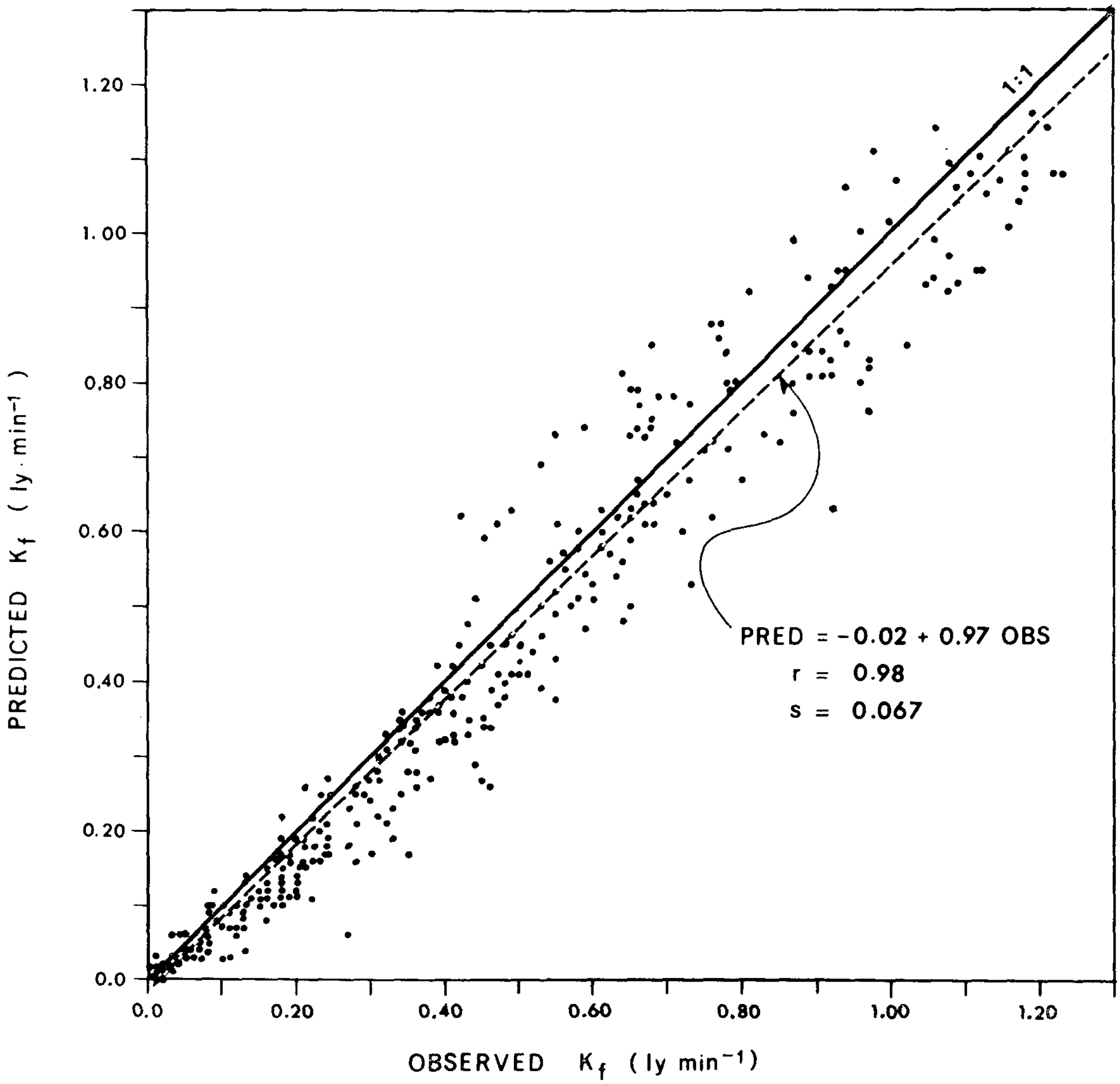

FIG. 7. Predicted and observed values of solar radiation for a total of 368 hr.

open locations, although this seems unreasonable in a qualitative assessment of the solarimeter positions, and unfortunately the present data does not permit a quantitative assessment of the sample's representativeness.

Fig. 7 shows the relationship between the predicted and observed values for a total of 368 hr. Linear regression analysis gives

$$\text{predicted} = -0.02 + 0.97 \text{ observed}, \qquad (10)$$

with a correlation coefficient of 0.98 and a standard error of 0.07 ly min^{-1}. Thus, the model tended to produce underestimates through the entire range of radiation conditions, but the error exceeded 10% of the observed value only when the observed flux was less than about 0.25 ly min^{-1}. The results for 12 daily totals (Fig. 8) are similar; the mean daily total was 388 ly day^{-1} and the average underestimate represented 7% of the mean or 27 ly day^{-1}.

The relatively low standard error of the prediction is very encouraging since a regression analysis between the observed hourly values of K_f and $(Q+q)$ at Schefferville gives

$$K_f = 0.00 + 0.85(Q+q), \qquad (11)$$

with a standard error of 0.08 ly min^{-1}. A similar analysis between the observed values at Schefferville and at the Wishart Creek open hill site shows a standard error of 0.10 ly min^{-1}. Thus, the scatter between the hourly observed and calculated values of K_f can be attributed primarily to the differences in solar radiation that occur over a distance of 5 mi. The standard error for daily totals can be expected to be smaller (as shown in Fig. 8)

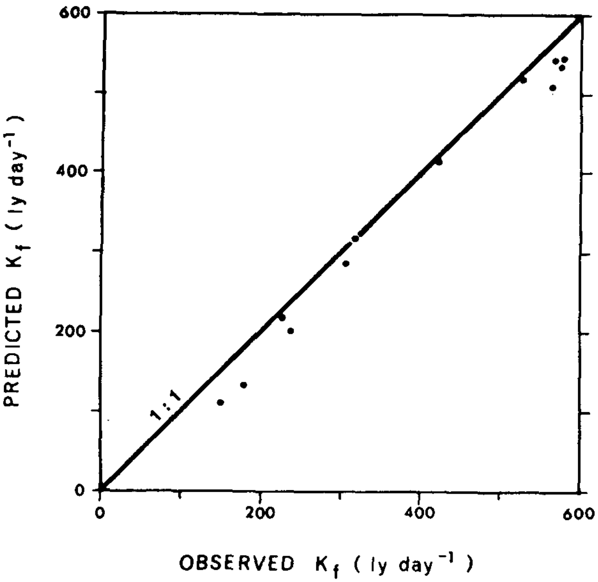

FIG. 8. Predicted and observed values of solar radiation for 12 days.

because differences in the cloud patterns would tend to cancel over the period of a day, and, for this distance, the analysis of Wilson and Petzold (1972) indicates that the standard error should be about 31 ly day^{-1}. Errors in the predictions fall within these limits and well within the observed difference between the open and woodland as indicated by (11).

5. Conclusions

The success of the predictions in this first test indicates that the model's simplicity is justified. It must be recognized, however, that simplicity is possible because the forest in question has an open structure. If the model were to be applied to forests of significantly different density, then it might be necessary to consider the effect of overlapping images and to allow for penetration of a small amount of diffuse radiation through the tree branches. It might also be necessary to change the logarithmic tree profiles, particularly where there is a recognizable trunk space without branches near the ground.

The mathematical model of view factors is a valuable alternative to the photographic technique since it permits analysis from physical arguments, and it is interesting to note that in this case the radiation income was virtually unaffected by trees which were removed by more than about four times the mean distance between the trees. The model also permits calculations of view factor changes produced by snow melting, and for sites where the special photographs have not been taken. The three tree measurements required by the model were determined here by ground-based sampling, but low-altitude air photographs could be used for larger or inaccessible areas.

Acknowledgments. We wish to thank Dr. T. Dunne, Mr. J. FitzGibbon and Mr. A. Price for their suggestions concerning the model, and Dr. F. Nicholson, Director of the McGill Sub-Arctic Research Laboratory, for his help with the arrangement of the field work. This research was supported by the National Research Council of Canada and the Department of Education of the Province of Quebec.

REFERENCES

Federer, C. A., 1971: Solar radiation absorption by leafless hardwood forests. *Agric. Meteor.*, **9**, 3–20.

FitzGibbon, J., and T. Dunne, 1973: Photographic measurement of vegetation canopies for use in the computation of the radiation balance. *McGill Univ. Climat. Bull.*, **13**, 1–8.

Horowitz, J. L., 1969: An easily constructed shadow-band for separating direct and diffuse solar radiation. *Solar Energy*, **12**, 543–545.

Reifsnyder, W. E., and H. W. Lull, 1965: Radiant energy in relation to forests. *U. S. Dept. Agric. Tech. Bull.*, No. 1344, 111 pp.

——, G. M. Furnival and J. L. Horowitz, 1971: Spatial and temporal distribution of solar radiation beneath forest canopies. *Agric. Meteor.*, **9**, 21–37.

U. S. Army Corps of Engineers, 1956. *Snow Hydrology*. North Pacific Division, Corps of Engineers, Portland, Ore., 437 pp.

Wilson, R. G., and D. E. Petzold, 1972: Daily solar radiation differences between stations in southern Canada: A preliminary analysis. *McGill Univ. Climat. Bull.*, **11**, 11–22.